

Functionalization of edge reconstructed graphene nanoribbons by H and Fe: a density functional study

Soumyajyoti Halder,¹ Sumanta Bhandary,¹ Satadeep Bhattacharjee,¹ Olle Eriksson,¹ Dilip Kanhere,² and Biplab Sanyal¹

¹*Department of Physics and Astronomy, Uppsala University, Box 516, 75120 Uppsala, Sweden*

²*Department of Physics, Central University of Rajasthan, Bander Sindri Campus, Dist-Ajmer, Rajasthan-305801, India*

In this paper, we have studied functionalization of 5-7 edge-reconstructed graphene nanoribbons by ab initio density functional calculations. Our studies show that hydrogenation at the reconstructed edges is favorable in contrast to the case of unreconstructed 6-6 zigzag edges, in agreement with previous theoretical results. Thermodynamical calculations reveal the relative stability of single and dihydrogenated edges under different temperatures and chemical potential of hydrogen gas. From phonon calculations, we find that the lowest optical phonon modes are hardened due to 5-7 edge reconstruction compared to the 6-6 unreconstructed hydrogenated edges. Finally, edge functionalization by Fe atoms reveals a dimerized Fe chain structure along the edges. The magnetic exchange coupling across the edges varies between ferromagnetic and antiferromagnetic ones with the variation of the width of the nanoribbons.

I. INTRODUCTION

Graphene is a wonder material with many extraordinary electronic, mechanical and optical properties to be used in future technology^{1,2}. Moreover, the similarity between its properties and the phenomena observed in high energy physics has created enormous possibilities to test fundamental theories in quantum electrodynamics by table-top experiments. Apart from exploring the beautiful physics associated with the Dirac cones in the Brillouin zone, a perpetual interest exists in the chemical functionalization of graphene to realize new properties. One of the routes of chemical functionalization is through the creation of defects in graphene and hence, modification of its properties³⁻⁷. The other notable effort is to attach chemical species (H, F etc.) to graphene to open up band gaps by altering sp^2 bonds to sp^3 ones between C atoms⁸⁻¹⁰. Very recently, it has also been shown¹¹⁻¹³ that a combination of boron nitride and carbon in a two dimensional network can yield interesting electronic properties, e.g., opening of band gaps in an otherwise zero band gap semiconducting situation in pure graphene.

Graphene nanoribbons (GNRs) have attracted a lot of attention in the last few years as they are potential candidates for future nanoelectronics. It is well-known¹⁴ that armchair nanoribbons are semiconductors while the zigzag GNRs (ZGNRs) have magnetic edges coupled to each other antiferromagnetically to open up a gap. Band gap engineering as a function of the thickness of GNRs is an important study towards realizing tunable electronics¹⁵. Also, chemical functionalization of GNR edges to achieve novel properties is another strong motivation to study GNRs. Recent theoretical studies have reported the possibility of realizing zigzag and armchair type nanoribbons at the interface of graphene and graphane (hydrogenated graphene)¹⁶⁻¹⁹ demonstrating an interesting way of generating nanoribbons.

It has been proposed that apart from realizing the conventional and most abundant GNR edges, viz.,

zigzag and armchair, one may consider self reconstructed edges²⁰ where the hexagonal rings at the edges reconstruct to form pentagon-heptagonal pairs (reczag). This is similar to what has been observed as 5-7-5 Stone-Wales defects in bulk graphene. Calculations suggest that the total energy of a reconstructed edge is 0.35 eV/Å lower than that of a zigzag one. The presence of a reconstructed edge geometry has been confirmed in experiments²¹ using aberration corrected high resolution transmission electron microscopy. A recent review article²² has discussed about the formation of defective edges along with the folded ones where the adjacent edges of multilayered graphene can join to form closed loops. The discussions on the zigzag and reconstructed edges is very important from the point of view of magnetism at the GNR edges, which is a debatable issue. Recent density functional calculations²³ suggest that the single edge reconstructed GNRs show magnetism with metallic edges although the reconstructions allowed at both edges do not show any magnetism. Rodrigues *et al.*²⁴ have studied reconstructed zigzag nanoribbons decorated by Stone-Wales defects by tight-binding theory with the parameters extracted from first principles electronic structure calculations.

From the above discussions, it is clear that the formation of reconstructed edges can modify the properties of GNRs drastically. So, a thorough understanding of the properties of the edges is essential along with the possibilities of realizing novel properties due to chemical functionalization by adatoms or molecules²⁵. The motivation of this present work is to study of the properties of edge-functionalized reconstructed GNRs by ab initio calculations. We have focussed on the geometries and electronic structures of reczag edges of varying thicknesses, their stability at finite temperatures under hydrogenation. Finally, we have exploited the possibility of realizing magnetism by decorating the edges with Fe atoms. In this regard, electronic structure, magnetic exchange coupling across the edges and the stable geometries of Fe chains

at the edges have been studied.

II. COMPUTATIONAL DETAILS

First principles spin-polarized density functional calculations were performed using a plane-wave projector augmented wave (PAW) method based code, VASP^{26,27}. The generalized gradient approximation (GGA) as proposed by Perdew, Burke and Ernzerhof (PBE)³⁰ was used for the exchange-correlation functional. We have considered different sizes of double edged reczag, which were infinite along the y axis. To create a sufficient vacuum in order to avoid the interactions within adjacent cells, unit cell dimensions along x and z axis were considered as 50 Å and 16 Å respectively. The electronic wave functions were expanded using plane waves up to a kinetic energy of 500 eV. The electron smearing used was Fermi smearing with a broadening of 0.05 eV. The energy and the Hellman-Feynman force thresholds were kept at 10^{-5} eV and 0.005 eV/Å respectively. All atomic positions were allowed to relax and the elemental cell was kept at a constant size during the optimization. For all electronic and ionic calculations, we used a $1 \times 60 \times 1$ *k* Monkhorst-Pack k-point mesh, whereas for phonon calculations, a $1 \times 79 \times 1$ mesh was used. The phonon frequencies and displacements were obtained using frozen phonon method²⁸. A few selected calculations for the geometry optimizations and electronic structures were repeated by using the Quantum Espresso code²⁹ using plane wave basis sets and pseudopotentials within GGA-PBE. We tested the convergence with respect to the basis-set cutoff energy and a value of 80 Ry. was considered for all results shown in this paper. The other parameters were similar to those used in VASP calculations. We found out that the results obtained by the two codes are quite similar.

In all our calculations, we have kept the unit cell vectors fixed. However, we have tested cell relaxation for 4-rows 2H terminated reczag GNR, as in this case, the effect of cell relaxation is expected to be the largest. From our calculations, we find that the change in unit cell length along the periodic direction (y) is less than 3 % and along x direction, it is 0.7 %. The maximum change in the C-C bond length is 1.8 % whereas the maximum change in the H-C-H bond angle is only 0.2 %. Our results are not affected by these changes due to cell relaxation.

III. RESULTS

A. Edge termination by H

The dangling bonds of edge carbon atoms are extremely reactive and need to be saturated. Among the several possible ways of edge termination, we concentrate on hydrogen termination at the edges as this seems to be one of the most stable configurations due to its planar

structure. We have considered the reczag edge termination by one (1H) and two (2H) hydrogen atoms attached to each edge carbon atom for nanoribbons of width 4 to 12 rows. Figure 1 shows the optimized geometry of a reczag edge with 2H termination.

The C atoms in the middle of the ribbons rearrange themselves after geometry optimization and the bond lengths come out to be very close to the C-C bond distances of bulk graphene (1.42 Å). However, the creation of edge reconstruction and H termination significantly changes the C-C bond distances near the edge. In a bare reczag edge without H termination, the edge carbon atoms form a triple bond with a bond length of 1.25 Å. When this edge is terminated by 1H, this bond length increases to 1.43 Å. Both bare reczag edge and the 1H terminated one have planar structures. In the case of 2H termination, the sp^2 planar structure becomes buckled, making an sp^3 like structure with an angle 102° between the H and edge carbon atoms. The C-C bond length increases further to 1.58 Å. However, the C-C bond length of 1.42 Å in sp^2 bonded graphene is recovered in the middle of the ribbon. The edge carbon atoms are displaced from the plane of the ribbon with one C atom shifting upwards and one downwards. H atoms attached to these two carbon atoms also change their orientation to give rise to a twisted geometry as shown in figure 1. To investigate the reason of twisting we have done Γ point (long wavelength) phonon calculations of 2H terminated reczag edge using frozen phonon method²⁸. We find that the structure with 2 H atoms vertically placed on one another and connected to the edge C atom is not stable, showing two unstable modes involving the displacement of H atoms away from the vertical position. For 2H termination, we therefore relaxed the structure again with these two unstable modes frozen. The relaxed structure was stable and a twisted geometry (shown in figure 1) was obtained due to the freezing of the above mentioned modes. It is obvious that the edge sp^3 structure has substantial effects on the whole part of ribbons with smaller widths whereas the structural distortion is not prominent in the middle of the wider ribbons.

For the termination of edges with 2 H atoms per C, the formation energies have been defined as $E_f = E(G2H) - [E(G1H) + n * E(H_2)]$, where $E(G2H)$ and $E(G1H)$ are the total energies for reconstructed graphene nanoribbons' edges terminated with 1H and 2H atoms per edge, respectively. $E(H_2)$ is the calculated energy for a H_2 molecule in the gas phase and n is the number of H_2 molecules used to compensate the uneven number of H atoms.

The calculated formation energies indicate that 2H terminated edge is probable to form. Also it is observed (data not shown) that the formation energies saturate after a width of eight rows as reported before³¹ for a unreconstructed edge zigzag nanoribbon. Moreover, our calculation shows that the termination with H atoms will be spontaneous at T=0K. We have done test calculations by freezing the edge carbon bond lengths. The edge hydro-

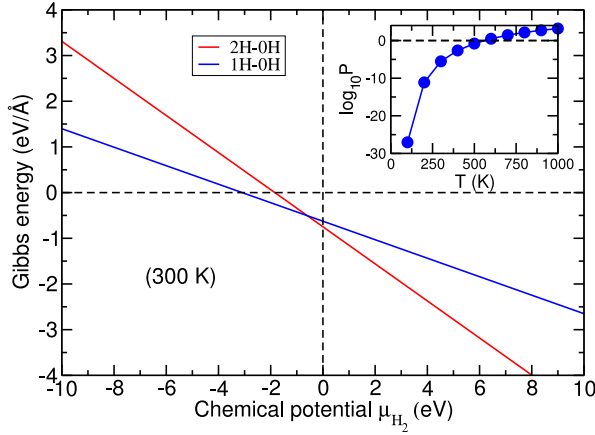
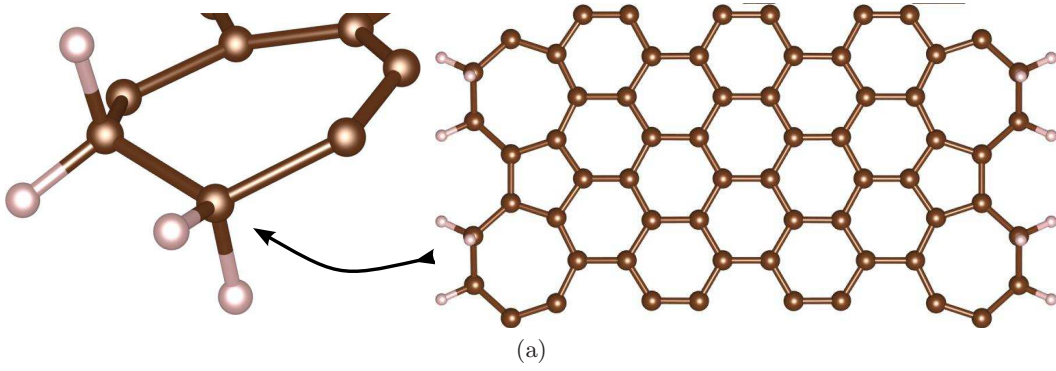


FIG. 1. (Color online) (a) Reconstructed edge GNR with 2H termination. Brown (dark in print) balls are C atoms and white (light in print) balls indicate H atoms. The close-up of the edge structure is also shown; (b) Gibbs free energy calculated for 12 rows-reczag. Both 1H and 2H terminations with respect to bare reczag are presented. In the inset, transition pressures as a function of temperatures are shown. P^0 is the reference pressure taken to be 0.1 bar.

generation seems to be difficult if the C-C bond lengths are not allowed to relax. Once the full geometry optimization is allowed, edge hydrogenation becomes probable. For the reconstructed edges, we find that a spontaneous formation of 2H terminated edges is possible rather than the 1H terminated ones for all widths. This is in sharp contrast with the hydrogenation at the unreconstructed ZGNRs studied earlier³¹.

In order to investigate the influence of finite temperature/elevated gas pressure, we have calculated Gibbs free energies as a function of the chemical potential of the hydrogen molecule, according to the following formula given by Wassmann *et al.*³².

$$G_{H_2} = \frac{1}{2L} [E_{H_2} - (\frac{N_H}{2})\mu_{H_2}]$$

$$G_{H_1} = \frac{1}{2L} [E_H - (\frac{N_H}{2})\mu_{H_2}]$$

$$E_{H_2} = E(G2H) - [E(G0H) + 4E(H_2)]$$

$$E_H = E(G1H) - [E(G0H) + 2E(H_2)]$$

$$\mu_{H_2} = H^0(T) - H^0(0) - TS^0(T) + k_B T \ln(\frac{P}{P^0})$$

In the above equations, μ_{H_2} , H , S , P and k_B are the chemical potential, enthalpy, entropy, pressure and Boltzmann constant respectively and N_H is the number of H atoms attached at the edge. The values for the entropies and enthalpies are taken from the tabular data presented in Ref.³³. P^0 is the reference pressure taken to be 0.1 bar according to the tabular data. $E(G2H)$, $E(G1H)$, $E(G0H)$ and $E(H_2)$ are total energies for 2H, 1H and bare reconstructed nanoribbons and hydrogen molecule respectively. The results are shown in figure 1

for 300 K. The Gibbs free energy is normalized by $2L$, where L is unit cell length. The stability of 2H and 1H terminated reconstructed nanoribbons is shown with respect to bare reconstructed nanoribbons. The zero temperature calculation shows that they are always favored compared to the bare nanoribbons. Also, 2H terminated ribbons are more stable than the 1H ones. With the inclusion of temperature and pressure effects, it is observed that at low pressure, 1H terminated edge can be stabilized over 2H terminated edge but after a certain pressure, 2H edge becomes more stable. We call this cross over point as the transition point. The pressure required to reach this transition point increases with temperature as shown in the inset of figure 1. The values of transition point pressures also suggest the possibility of the formation of a 2H terminated reczag edge at room temperature and ambient pressure.

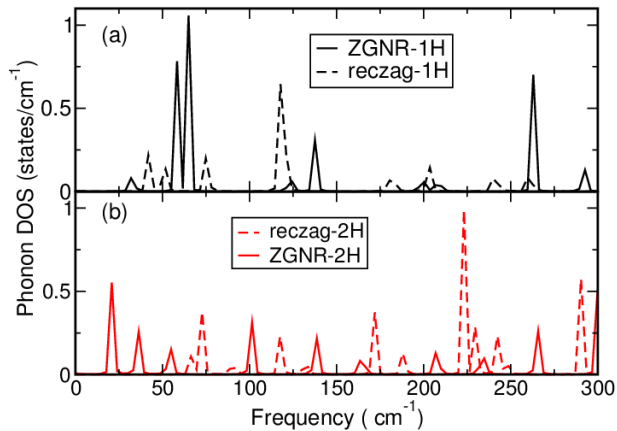


FIG. 2. (Color online) Zone center phonon DOSs plotted as a function of frequency for (a) 1H terminated ZGNR and reczag structures and (b) 2H terminated ZGNR and reczag structures.

The calculated electronic structures (data not shown) for 1H and 2H terminations show the presence of finite density of states at Fermi energy originating mostly from the p_z orbitals of the C atoms next to the edge C atoms. However, the magnetic moment is lost due to the saturation of C-C bonds at the edges, as seen earlier^{20,32,34}. Unreconstructed ZGNR with 1H and 2H terminated edges have finite magnetic moments and metallicity^{14,31}. In contrast to those, both 1H and 2H terminated reczag edges are non magnetic in the present case.

Now, we show the comparison of the phonon densities of states of 1H and 2H terminated unreconstructed and reconstructed edge structures. The results are shown in figure 2 where only optical phonons are displayed. From the figure it is clear that due to edge reconstruction, the lowest optical phonon modes are hardened. This hardening is however enhanced in the case when the edge is

terminated with 2H compared to that of 1H.

B. Edge termination with Fe

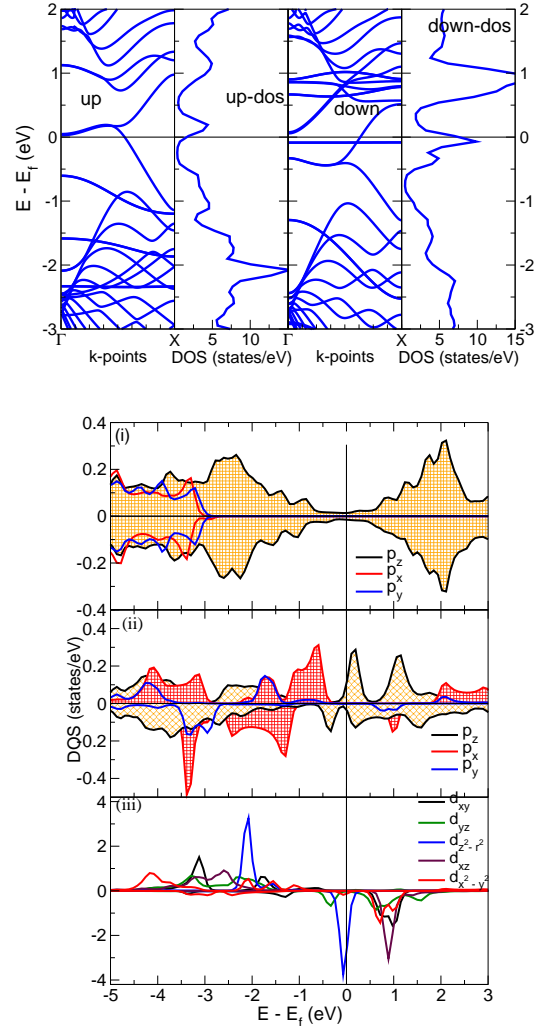


FIG. 3. (Color online) (left) Total DOSs and band structures for an Fe decorated 12 rows reczag edge. Both spin-up and spin-down states are shown. (Right) Spin-polarized site and orbital projected DOSs for (a) C atoms in the middle of the ribbon, (b) edge C atoms and (c) Fe atom.

The edge reconstruction destroys the magnetism of C atoms at the edges as the flat bands near or on Fermi level for unreconstructed GNRs are now highly dispersive due to increased hybridization. To introduce magnetism and also to observe magnetic interaction through graphene lattice, we decorated the edges with Fe atoms. Our geometry optimization shows that the Fe atom placed in between two heptagons is favorable over top-hexagon or top-pentagon positions by at least 27 meV/C atom. The

calculated formation energies of Fe terminated reczag edge are around 2.6 eV when the chemical potential of Fe is taken as the same as bulk bcc Fe. The formation energy E_f of a metal atom at the edge, is defined as $E_f = E(\text{Met}_N + \text{reczag}) - [N * E(\text{Met}) + E(\text{reczag})]$, where $E(\text{Met}_N + \text{reczag})$ is the total energy of geometry optimized Metal+reconstructed edge graphene nanoribbon, $E(\text{reczag})$ is the total energy for the optimized geometry of reconstructed edge GNR and $E(\text{Met})$ is the chemical potential of the metal calculated in its bulk phase. N is the number of metal atoms in the unit cell. It should be noted that a recent paper³⁶ reports a negative formation energy (indication of spontaneous formation) for Fe decoration at the zigzag or armchair edges when the chemical potential is taken from Fe in the atomic phase. So, the formation of Fe decorated edges highly depends on the Fe reference level.

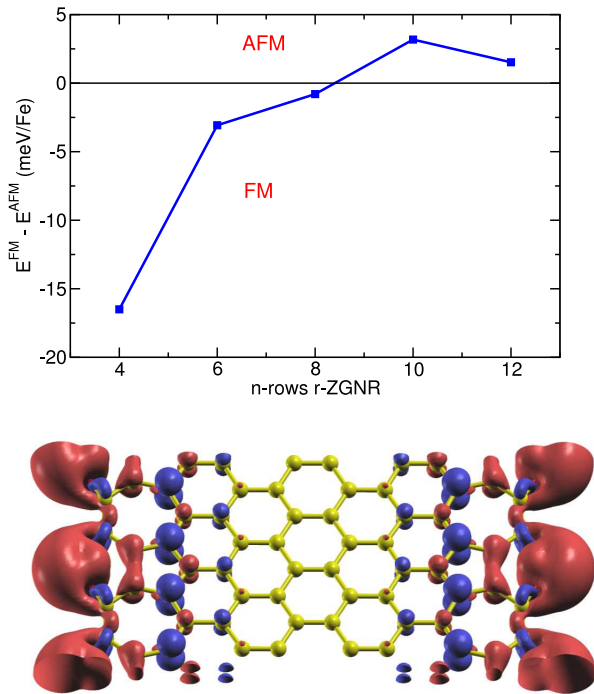


FIG. 4. (Color online) (top) Inter-edge exchange coupling (total energy difference between FM and AFM coupling across the edges) plotted as a function of ribbon width, (bottom) Spin density isosurfaces of 8-rows Fe doped reczag edge for a FM coupling across the edges. Red and blue colors represent spin-up and spin-down densities respectively.

Figure 3 shows the band structure and DOSs for an Fe edge-decorated 12 rows reczag edge. The spin down channel shows a localized peak in the total DOS (non dispersive band in the band structure plot) just below the Fermi level, contributed by Fe. The orbital projected DOSs on Fe (shown in panel (c) at the right of Figure 3) clearly indicate that this localized peak has a $d_{z^2-r^2}$

character in the spin-down channel. The spin-up channel of Fe is completely filled and has a negligible contribution within 2 eV below the Fermi level. The dispersive states in this energy range in the band structure arise mainly from edge C atoms. Projected DOSs on C atoms at the edge (panel (b)) are quite different from the ones in the middle (panel (a)) of the nanoribbon. The dominance of p_z character within a considerable energy range around Fermi level in panel (a) is similar to what is observed for bulk graphene. The edge C atoms are spin-polarized and a strong contribution of in-plane p_x and p_y orbitals are seen in the similar energy range.

If we look at the structural changes owing to the addition of Fe atoms, it has effect on heptagons only as we have seen for the hydrogenated reczag edges. But the effect of Fe on the graphene lattice is longer ranged as evident from the spin density isosurfaces shown in figure 4. The local moment on Fe is around $3.5 \mu_B$ for all widths considered. The Fe moments are quite robust and they are independent of width as well as on the exchange coupling (FM or AFM) across the two edges of the nanoribbons. The closest C atoms, to which Fe is bonded, have induced moments antiparallel to the Fe ones and same for their same sublattice carbons, whereas other sublattice carbon atoms have in phase magnetization. As we travel towards the center of the ribbon, this effect is decreased. The opposite magnetization in different sublattices is clearly visible throughout the ribbon for the AFM coupled edges whereas for FM coupling, the magnetization disappears in the middle of the nanoribbon due to the cancellation of induced moments.

We have done a calculation to check the possibility of monohydrogenation of a 12 rows reczag GNR already functionalized with Fe. We have found that it's comparatively less favorable (formation energy of -0.29 eV compared to -0.63 eV in the absence of Fe) to have a 1H termination in the presence of Fe. This is expected as Fe is already bonded at the edge and the H atom does not have enough room for bonding as it was possible in the absence of Fe.

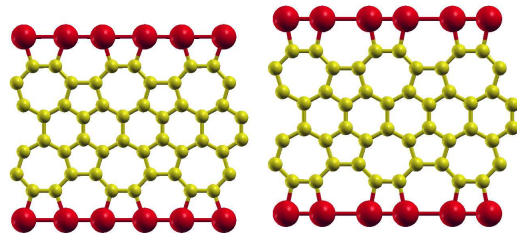


FIG. 5. (Color online) The structures of two dimerized chains indicated as Dimer 1 (left) and Dimer 2 (right) in Table I. In the figure, red and yellow balls indicate Fe and C atoms respectively.

The exchange coupling (measured by the total energy difference between FM and AFM coupling across the

Dimer	ΔE (eV)	Fe-Fe distance 1 (Å)	Fe-Fe distance 2 (Å)	moment (μ_B)
1	-0.23	2.61	2.30	2.94
2	-0.29	2.77	2.14	2.94

TABLE I. Formation energies (ΔE) of two types of Fe dimers in the chain with respect to non-dimerized structure. The corresponding bond lengths (short and long) of the Fe dimers are shown for the two structures shown in figure 5 along with the local magnetic moments at Fe sites.

edges) is plotted against the width of the nanoribbon and is shown in Figure 4. For 4 rows, there is a relatively strong FM coupling. With the increase in width, this coupling decreases and changes to an AFM one after 8 rows. The AFM coupling tends to decrease afterwards. Interesting features of interedge coupling has been reported recently³⁶ for Fe and Co decorated armchair nanoribbons, where an oscillatory exchange coupling has been observed. The analogy with interlayer exchange coupling in case of magnetic multilayers coupled through nonmagnetic layers³⁷ was made in that paper. The period of the coupling was analyzed in connection to Fermi surface nesting vectors.

Finally, we discuss the possibility of the formation of a dimerized Fe chain along the edges of the nanoribbons as this issue has been explored in case of unreconstructed 6-6 nanoribbons³⁶. This situation is different from the above discussions where the density of edge Fe atoms was considered to be lower. Here we allow the Fe atoms to bind to the edge C atoms of the heptagon in contrast to the previous case, where one Fe atom was allowed to sit in between the heptagons and hence, the Fe atoms were far enough to have the possibility of dimerization. To study the dimerization, we started the geometry optimization from two different configurations of Fe dimers and have obtained the ground state geometries as shown in figure 5. One can observe two types of dimer structures, one formed between the Fe atoms connected to the carbon atoms of a heptagon (second structure of figure 5) and the second type is formed between the Fe atoms connected to carbon atoms belonging to adjacent heptagons. Both the dimers are stable with respect to non-dimerized Fe termination. Table I shows the energetics, structure and magnetism for the two cases. It is evident that Fe dimers connected to the same heptagon is favorable over the other one by an energy of 0.06 eV. The bond length of this dimer comes out to be 2.14 Å whereas the other structure yields a bond length of 2.3 Å. The local magnetic moments on Fe are same for these two structures and are close to 3 μ_B . It is interesting to note that the moments are reduced compared to the non-dimerized Fe chains, where the hybridization between the Fe-d orbitals was weaker due to larger separations. The electronic structure and corresponding magnetic exchange coupling for these dimerized structures will be discussed in a future communication.

IV. CONCLUSIONS

In this paper, chemical functionalization at the edges of reconstructed zigzag graphene nanoribbons has been studied by ab initio density functional theory. Reconstructed edges do not show any magnetism and have a metallic behavior. From our calculations, it is seen that both single and dihydrogenated reczag edges are probable to form, as observed in previous theoretical calculations.. Unlike unreconstructed ZGNRs, dihydrogenation is always favorable over monohydrogenated reczag edges, independent of the width of the nanoribbons under ambient conditions. We have also shown that at finite temperatures, the hydrogen pressure dictates the formation of mono- or di- hydrogenated edges. Our phonon calculations reveal a peculiar geometry at the dihydrogenated edges. Moreover, it has been found that the lowest optical phonon modes are hardened due to edge reconstruction. To render magnetism in reczag edges, we have decorated the edges by Fe chains. The interedge magnetic coupling varies between ferromagnetic and antiferromagnetic ones with the variation of the width of the nanoribbons with robust localized moments residing at the Fe sites. Finally, we show that the Fe atoms in the chain along an edge prefer to be in a dimerized configuration.

ACKNOWLEDGEMENTS

SH would like to acknowledge Indo-Swiss grant for financial support (No: INT/SWISS/P- 17/2009). BS acknowledges Swedish Research Links programme under VR/SIDA, Göran Gustafssons Stiftelse, Carl Tryggers Stiftelse and KOF initiative by Uppsala University for financial support. We thank SNIC-UPPMAX, SNIC-NSC and SNIC-HPC2N computing centers under Swedish National Infrastructure for Computing (SNIC) for granting computer time. O.E. acknowledges support from ERC and the KAW foundation.

REFERENCES

- ¹A. K. Geim, K. S. Novoselov, The rise of graphene, NATURE MATERIALS 6 (2007) 183.
- ²A. H. Castro Neto, F. Guinea, N. M. R. Peres, K. S. Novoselov, A. K. Geim, The electronic properties of graphene, Rev. Mod. Phys. 81 (2009) 109.
- ³V. A. Coleman, R. Knut, O. Karis, H. Grennberg, U. Jansson, R. Quinlan, B. C. Holloway, B. Sanyal, O. Eriksson, Defect formation in graphene nanosheets by acid treatment: an x-ray absorption spectroscopy and density functional theory study, Journal of Physics D: Applied Physics 41 (2008) 062001.
- ⁴B. Sanyal, O. Eriksson, U. Jansson, H. Grennberg, Molecular adsorption in graphene with divacancy defects, Phys. Rev. B 79 (2009) 113409.

- ⁵S. H. M. Jafri, K. Carva, E. Widenkvist, T. Blom, B. Sanyal, J. Fransson, O. Eriksson, U. Jansson, H. Grennberg, O. Karis, R. A. Quinlan, B. C. Holloway, K. Leifer, Conductivity engineering of graphene by defect formation, *Journal of Physics D: Applied Physics* 43 (2010) 045404.
- ⁶S. Bhandary, S. Ghosh, H. Herper, H. Wende, O. Eriksson and B. Sanyal, Graphene as a Reversible Spin Manipulator of Molecular Magnets, *Phys. Rev. Lett.* 107 (2011) 257202.
- ⁷E. Holmström, J. Fransson, O. Eriksson, R. Lizarraga, B. Sanyal, S. Bhandary, and M. I. Katsnelson, Disorder-induced metallicity in amorphous graphene, *Phys. Rev. B* 84 (2011) 205414.
- ⁸J. O. Sofo, A. S. Chaudhari, G. D. Barber, Graphane: A two-dimensional hydrocarbon, *Phys. Rev. B* 75 (2007) 153401.
- ⁹D. C. Elias, R. R. Nair, T. M. G. Mohiuddin, S. V. Morozov, P. Blake, M. P. Halsall, A. C. Ferrari, D. W. Boukhvalov, M. I. Katsnelson, A. K. Geim, K. S. Novoselov, Control of graphene's properties by reversible hydrogenation: Evidence for graphane, *Science* 323 (2009) 610.
- ¹⁰M. Klintonberg, S. Lebègue, M. I. Katsnelson, O. Eriksson, Theoretical analysis of the chemical bonding and electronic structure of graphene interacting with group ia and group viia elements, *Phys. Rev. B* 81 (2010) 085433.
- ¹¹L. Ci, L. Song, C. Jin, D. Jariwala, D. Wu, Y. Li, A. Srivastava, Z. F. Wang, K. Storr, L. Balicas, F. Liu, P. M. Ajayan, Atomic layers of hybridized boron nitride and graphene domains, *NATURE MATERIALS* 9 (2010) 430.
- ¹²J. Zhu, S. Bhandary, B. Sanyal, H. Ottosson, Interpolation of atomically thin hexagonal boron nitride and graphene: Electronic structure and thermodynamic stability in terms of all-carbon conjugated paths and aromatic hexagons, *The Journal of Physical Chemistry C* 115 (2011) 10264.
- ¹³P. P. Shinde and V. Kumar, Direct band gap opening in graphene by BN doping: Ab initio calculations, *Phys. Rev. B* 84 (2011) 125401.
- ¹⁴Y.-W. Son, M. L. Cohen, S. G. Louie, Half-metallic graphene nanoribbons, *NATURE* 444 (2007) 347.
- ¹⁵M. Y. Han, B. Özyilmaz, Y. Zhang, P. Kim, Energy band-gap engineering of graphene nanoribbons, *Phys. Rev. Lett.* 98 (2007) 206805.
- ¹⁶A. K. Singh, B. I. Yakobson, Electronics and Magnetism of Patterned Graphene Nanoroads, *Nano Lett.* 9 (2009) 1540.
- ¹⁷P. Chandrachud, B. S. Pujari, S. Haldar, B. Sanyal, D. G. Kanhere, A systematic study of electronic structure from graphene to graphane, *Journal of Physics: Condensed Matter* 22 (2010) 465502.
- ¹⁸S. Haldar, D. Kanhere, B. Sanyal, *Phys. Rev. B*, Magnetic impurities in graphane with dehydrogenated channels, *Phys. Rev. B* 85 (2012) 155426.
- ¹⁹C. D. Reddy, Q. H. Cheng, V. B. Shenoy, Y. W. Zhang, Interfacial properties and morphologies of graphene-graphane composite sheets, *J. Appl. Phys.* 109 (2011) 054314.
- ²⁰P. Koskinen, S. Malola, H. Häkkinen, Self-passivating edge reconstructions of graphene, *Phys. Rev. Lett.* 101 (2008) 115502.
- ²¹Ç. Ö. Girit, J. C. Meyer, R. Erni, M. D. Rossell, C. Kisielowski, L. Yang, C.-H. Park, M. F. Crommie, M. L. Cohen, S. G. Louie, A. Zettl, Graphene at the edge: Stability and dynamics, *Science* 323 (2009) 1705.
- ²²X. Jia, J. Campos-Delgado, M. Terrones, V. Meunier, M. S. Dresselhaus, Graphene edges: a review of their fabrication and characterization, *Nanoscale* 3 (2011) 86.
- ²³S. Dutta, S. K. Pati, Edge reconstructions induce magnetic and metallic behavior in zigzag graphene nanoribbons, *Carbon* 48 (2010) 4409.
- ²⁴J. N. B. Rodrigues, P. A. D. Gonçalves, N. F. G. Rodrigues, R. M. Ribeiro, J. M. B. Lopes dos Santos, N. M. R. Peres, Zigzag graphene nanoribbon edge reconstruction with Stone-Wales defects, *Phys. Rev. B* 84 (2011) 155435.
- ²⁵Vanin et al, *PRB* 82, 195411 (2010); Ramasubramanian et al, *J. Appl. Phys.* 111, 054302 (2012)).
- ²⁶G. Kresse, J. Hafner, Ab initio molecular dynamics for liquid metals, *Phys. Rev. B* 47 (1993) 558.
- ²⁷G. Kresse, J. Furthmüller, Efficient iterative schemes for ab initio total-energy calculations using a plane-wave basis set, *Phys. Rev. B* 54 (1996) 11169.
- ²⁸K. Kunc, R. M. Martin, Density-functional calculation of static and dynamic properties of GaAs, *Phys. Rev. B* 24 (1981) 2311.
- ²⁹P. Giannozzi *et. al.*, URL <http://www.quantum-espresso.org>
- ³⁰J. P. Perdew, K. Burke, M. Ernzerhof, Generalized gradient approximation made simple, *Phys. Rev. Lett.* 77 (1996) 3865.
- ³¹S. Bhandary, O. Eriksson, B. Sanyal, M. I. Katsnelson, Complex edge effects in zigzag graphene nanoribbons due to hydrogen loading, *Phys. Rev. B* 82 (2010) 165405.
- ³²T. Wassmann, A. P. Seitsonen, A. M. Saitta, M. Lazzeri, F. Mauri, Structure, stability, edge states, and aromaticity of graphene ribbons, *Phys. Rev. Lett.* 101 (2008) 096402.
- ³³J. M. W. Chase, NIST thermochemical tables, *J. Phys. Chem. Ref. Data*, Monog. 9 (1998).
- ³⁴P. Koskinen, S. Malola, H. Häkkinen, Evidence for graphene edges beyond zigzag and armchair, *Phys. Rev. B* 80 (2009) 073401.
- ³⁵R. Gillen, M. Mohr, J. Maultzsch, C. Thomsen, Lattice vibrations in graphene nanoribbons from density functional theory, *physica status solidi (b)* 246 (2009) 2577.
- ³⁶Y. Wang, H.-P. Cheng, Interedge magnetic coupling in transition-metal terminated graphene nanoribbons, *Phys. Rev. B* 83 (2011) 113402.

³⁷P. Bruno and C. Chappert, Ruderman-Kittel theory of oscillatory interlayer exchange coupling, Phys. Rev. B 46 (1992) 261.